ChemComm

Accepted Manuscript

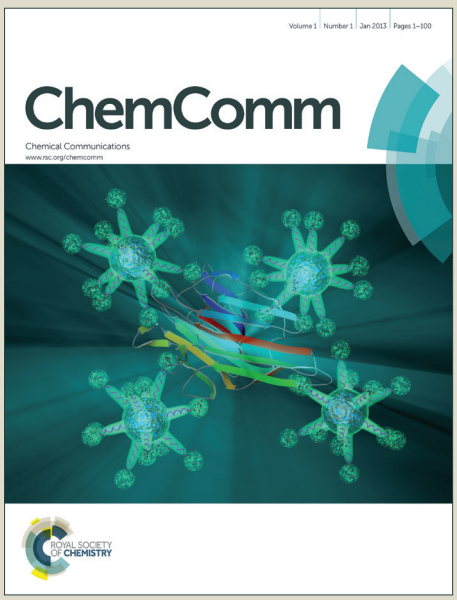

ROYAL SOCIETY OF CHEMISTRY

www.rsc.org/chemcomm

Cite this: DOI: 10.1039/c0xx00000x

www.rsc.org/xxxxxx

COMMUNICATION TYPE

Quantum dot/ methylene blue FRET mediated NIR fluorescent nanomicelles with large Stocks shift for bioimaging†

Li Li,‡ Jianbo Liu,‡ Xiaohai Yang, Zhihong Peng, Wei Liu, Jianguo Xu, Jinlu Tang, Xiaoxiao He,* Kemin Wang*

Received (in XXX, XXX) Xth XXXXXXXXX 200X, Accepted Xth XXXXXXXXX 200X

DOI: 10.1039/b000000x

Here we present a novel large Stokes shifting NIR fluorescent nanomicelle through encapsulation of quantum dot/ methylene blue FRET pair, which is employed as an excellent contrast reagent for NIR fluorescent bioimaging.

Near infrared (NIR) fluorescent imaging has become a promising technique in preclinical studies of human disease detection and treatment since they allow for bioimaging with minimal autofluorescence from biological samples, reduced light scattering, and high tissue penetration.[1,2,3,4] However, the direct employment of NIR fluorophores for biomedical imaging is still challenging for some limitations.[5,6,7] The small organic fluorophores generally exhibit low fluorescent intensity and photobleaching thresholds which constrain their effectiveness in long-term tracking of physiological behaviors.[8,9,10] Besides, most NIR dyes, such as polymethine cyanine dyes, have a small Stokes shift, which can cause self-quenching and crosstalk between the excitation light and the emitting signals.[11,12,13] Therefore, the development of bright NIR-emitting bioimaging nanoprobes is a significant challenge. To end this, some strategies were developed such as synthesis of NIR-emitting dyes with high stability and long Stocks shift, embedding NIR dyes in nanomicelles, design of fluorescence resonance energy transfer FRET (FRET) pair dyes.[14,15,16,17] FRET is the non-radiative transfer of energy from an excited fluorophore donor to another fluorophore acceptor. By comparison with a single fluorophore, FRET has a relatively larger gap between the excitation and emission and thus can significantly reduce crosstalk between the excitation light and the resulting fluorescence signals while imaging. FRET pair encapsulated nanomicelles, as a promising fluorescent contrast nanoprobe, are expected to overcome those above pivotal drawbacks, making them higher qualified contrast agents for bioimaging.[18,19] For example, Tan et. al. have developed barcoding silica NPs for multiplexed signaling by encapsulating different ratio of three dyes.[20,21] Law et. al. have prepared polymeric nanoparticles doped with DiD/DiR FRET pair for in vivo NIR imaging.[22] In our previous work, RuBpy and methylene blue FRET pair encapsulated fluorescent silica nanoparticles was developed as large Stokes shifting nanoprobe for in vivo NIR small animal imaging.[16] It is well known that semiconductor quantum dots (QDs) have unique photophysical properties of continuous absorption spectra, narrow and tunable emission, and high photostability, and have attracted widespread attentions in the fields of bioimaging, and especially, QDs can afford as an efficient donor in the developing of FRET nanoprobes.[23,24,25,26,27] However, to the best of our knowledge, the dyes-doped FRET QDs nanomicelles for vivo NIR imaging has not yet been reported.

Here, we report the development of a kind of large Stokes shifting fluorescent nanomicelles for NIR bioimaging by taking advantage of the highly efficient FRET between the QDs donor and methylene blue (MB) acceptor that embedded in the cetyltrimethylammonium bromide (CTAB) nanomicelles. As illustrated in Figure 1, the fluorescent QDs and NIR fluorescence dye of MB were selected as the FRET pair model and the MB was embedded in QDs nanomicelles through surfactant CTAB-assistant, evaporation induced microemulsion approach. FRET from QDs to MB happened within the nanomicelles, resulting in the formation of QDs/MB nanomicelles with strong NIR fluorescence and large Stokes shift (~202 nm). The nanomicelles possessed satisfied colloidal stability and photostability. The tremendous potential of these nanomicelles rendered them showed great promise in cell and vivo imaging applications.

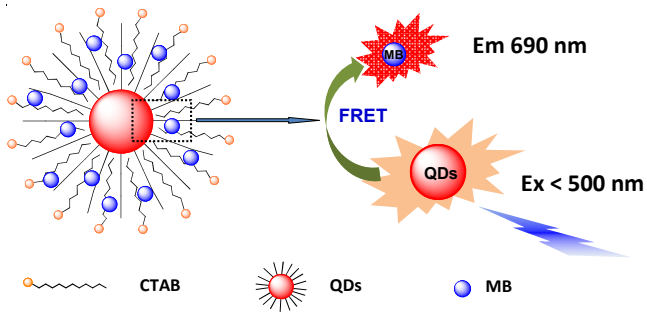

Figure 1. Schematic illustration of the NIR fluorescent QDs/MB nanomicelles with large Stocks shift. The QDs/ MB nanomicelles were fabricated through CTAB-assistant, evaporation induced microemulsion approach. FRET happened within the nanomicelles from donor QDs to MB acceptor.

The QDs/ MB nanomicelles were fabricated through typical surfactant-assistant, evaporation induced microemulsion approach. A concentrated solution of QDs in chloroform was added to an aqueous mixture of CTAB and MB under vigorous stirring to create an oil-in-water microemulsion. Chloroform evaporation during a heat course transfers the hydrophobic QDs into an aqueous phase. This interfacial process is driven by the hydrophobic vander Waals interactions between the primary alkane of the stabilizing ligand of octadecylamine and the secondary alkane of the surfactant, resulting in thermodynamically defined, interdigitated bilayer structures (Figure S1). The formed blue mother solution of nanomicelle suspension was finally centrifuged to remove any precipitates,

and the obtained QDs/MB nanomicelles could be well dissolved in deionized water.

To construct large Stokes shifting NIR fluorescent nanomicelles based on FRET, two fluorescent substances as FRET donor−acceptor pair were housed inside the water-in-oil microemulsion. Here, the reason we chose QDs emission at 630 nm and MB as the donor- acceptor pair is that emission spectrum of QDs shares a broad overlapping with the absorbance of MB, and MB emits bright fluorescence around 690 nm in the NIR window (Figure 2A). Under excitation at 488 nm, strong fluorescence was emitted from QDs, but low emission from sole MB. However, after encapsulation of the FRET pair in the nanomicelles, as expected, a strong emission peak at 690 nm in the NIR window could be detected. This emission peak of the QDs/MB nanomicelles is corresponding to that of the MB. This result clearly indicated an efficient FRET happened within the nanomicelles, and importantly, the Stokes shift of QDs/MB nanomicelles was greatly extended to about 202 nm (Figure 2B). Therefore, encapsulation of FRET pair in nanomicelles can efficiently overcome the problem of serious crosstalk and self-quenching for most NIR dyes with small Stokes shift.

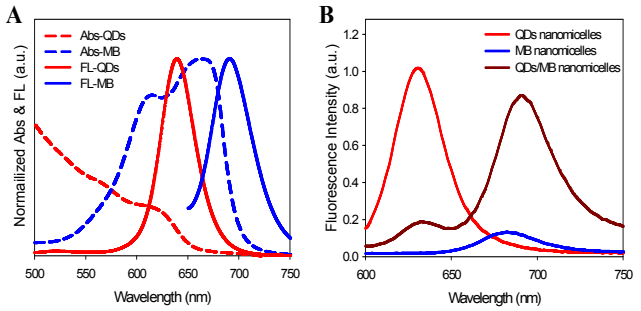

Figure 2. (A) Absorption (dashed) and fluorescent emission (solid) spectra of QDs (blue line) and MB (red line). (B) Fluorescence spectra of the QDs, MB and QDs/MB nanomicelles under the excitation of 488 nm.

The efficiency of FRET is greatly dependent on the concentration of the QDs donor and the MB acceptor. As increasing the concentration of MB from 0 to 70 μM, a significant enhancement of MB fluorescence intensity at 690 nm accompanied by a gradual quenching of QDs was observed (Figure S2A). These fluorescence fluctuations of the QDs and MB further confirmed the FRET relationship between the donor and acceptor pairs. The FRET efficiency derived from the loss in QDs fluorescence at each concentration of MB was shown in Figure S2B, and a high FRET efficiency of 82.2% could be achieved at QDs concentration of 85 nM and MB at 35 μM. In this case, the fluorescence of QDs/MB nanomicelles were 5-fold intensity to that of the sole MB dyes (Figure S2B).

From the perspective of FRET theory, the FRET efficiency is highly influenced by FRET radius R_0 and the donor-acceptor distance. As for FRET, FRET radius R_0 is defined as the distance between the donor and acceptor that yields 50% energy-transfer efficiency. Spectral overlap integral (J) reflecting the degree of overlap of the donor emission spectrum with the acceptor absorption spectrum, was calculated around 1.39×10^{-17} M^{-1} cm^{-1} nm^4. Therefore, according to the spectral overlap and quantum yield of the QDs donor (61%), R_0 between QDs and MB can be further calculated as 10.8 Å with the help of the software Matlab (Supplement Information). Generally, a long R_0 can cause a high FRET efficiency, but the system of QDs and MB possessed a relative small FRET radius R_0. In this case, we inferred that the real distance of donor-acceptor played a significant role in the energy transfer process. Furthermore, the size and the morphology of the prepared QDs/MB nanomicelles were examined. As illustrated in Figure 3A, transmission electron microscopy (TEM) imaging demonstrated that most of the micelles were assembled to a layer and it was observed that the micelles were mostly spherical in shape with an average size around 6.8 nm in diameter. HRTEM also validated the results and single QDs could be even clearly discriminated (Figure 3B). Dynamic light scattering (DLS) were also used to determine the size of the micelles. From the perspective of number distribution, the average hydrodynamic diameter (D_h) value was determined as 6.7 ± 4.3 nm, providing a strong indication of the small size of the nanomicelles. The DLS result was also consistent with that of TEM imaging. The size was also equivalent to the single QD encapsulated nanomicelles. Thus, it was concluded that MB was embedded in small QDs nanomicelles with several nanometers dimension, resulting in a strong FRET between the donor-acceptor pairs. Thereby, the FRET nanomicelles with strong NIR fluorescence and large Stocks shift is of great promise for cellular labeling and fluorescence imaging applications.

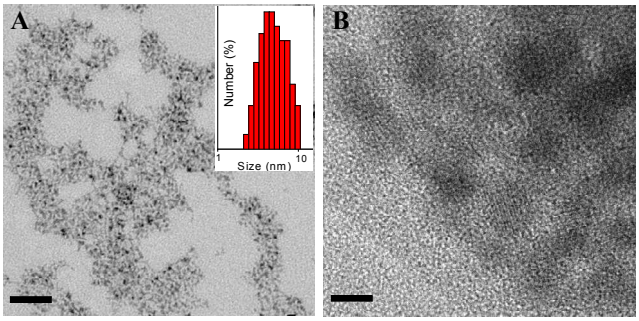

Figure 3. (A) TEM imaging and hydrodynamic diameters (inset) of the QDs/MB nanomicelles. Bar: 50 nm. (B) HRTEM of the QDs/MB nanomicelles. Bar: 5 nm.

Before the bioimaging application, the colloidal stability and photostability of FRET nanomicelles were thoroughly investigated. The colloidal stability of the FRET nanomicelles in different buffer media was investigated. It was observed that the nanomicelles can be well dispersed in PBS, Tris-HCl and HEPES buffer solutions at pH 7.4 (Figure S3). After store for 5 days, no obvious aggregates or precipitation could be observed. Besides, the thermal stability of the FRET nanomicelles were studied at 20 °C, 40 °C and 60 °C by investigating the variation of hydrodynamic size. The size of the QDs/MB nanomicelles showed no obvious alteration (Figure S4), which implied that the nanomicells were stable at different temperature. We believe the strong hydrophobic Vander Waals interactions between the stabilizing ligand of QDs and the hydrocarbons of the surfactant may endow the nanomicelles with high thermodynamically stable nanostructure. It is worth noting that the FRET nanomicelles can be also well dispersed in full mouse serum. But after the nanomicelles were incubated in full mouse serum for a period time, tiny amounts of dye would be leaked from the nanomicelles. As shown in Figure 4A, the fluorescence intensity of the QDs/MB nanomicelles were decreased about 10.1% after incubation for 5 h in full mouse serum. In the FRET nanomicelles, MB was embedded in the interior of the micelles is mainly because of high partition coefficient of the dye (log K_{ow} 5.85).[28] There were a plent of organic matter in the full mouse serum, so it was inevitable that some dye will be leaked and redistributed when the nanomicelles were dispersed in serum. In addition, the QDs/MB nanomicelles prepared in this work also have excellent

photostability, after continuously exposure to UV light for 5 h, no significant photobleaching can be observed for QDs/MB nanomicelles, while 42.9% the fluorescence attenuated for the MB nanomicelles (Figure 4B). This result indicated that alkane stabilizer around the nanomicelles could effectively prevent the photobleaching of dyes. The enhanced fluorescence intensity and photobleaching resistance of QDs/MB nanomicelles might be expected as a novel NIR fluorescent contrast agent for biological imaging application.

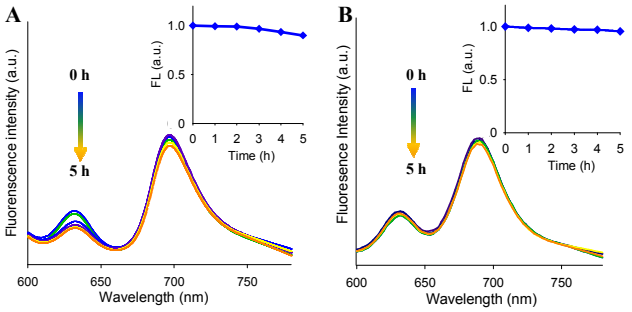

Figure 4. (A) Fluorescence intensity variation of QDs/MB nanomicelles in full mouse serum for a period time. (B) The fluorescence spectra of QD/MB (solid) nanomicelles and MB (dash) at excitation 488 nm after exposure to UV irradiation with 365 nm.

The nanomicelles with satisfied colloidal stability and photostability showed great promise in cell imaging application. The FRET nanomicelles were incubated with tumor HepG2 cell and the real time course of cellular uptake was investigated using laser confocal scanning microscopy. It was revealed that after addition of the nanomicelles into cell media, a tiny luminescence appeared in 10 min, and a strong fluorescence can be observed in 20 min (Figure 5 and Figure S5). The results suggested that the nanomicelles can be rapidly uptaken by cells. The rapid cell internalization may be from that the QDs/MB nanomicelles possessed highly positive charge around +41.7 mV (Figure S6), which provided a great convenience for cell imaging. In addition, the FRET fluorescence signals were also compared with the QDs and MB dye. As control, QDs nanomicelles without MB and MB nanomicelles without QDs were prepared respectively. It was found that under excitation of 488 nm, the fluorescence intensity and signal background ratio of QDs/MB nanomicelles was far larger than that of QDs and MB nanomicelles in the cell imaging. This was because of the efficient FRET between QDs and MB in the nanomicelles. The strong NIR fluorescence and high signal background ratio validated that QDs/MB nanomicelles can be a perfect nanoprobe for cell imaging. Meanwhile, the safety and toxicological issues of the QDs/MB nanomicelles were also examined. Here, an MTT assay was used for quantitative testing of the viability of cells for the nanomicelles. As shown in Figure S7, QDs/MB nanomicelles had no obvious effect on cell viability at concentrations ranging from 2.5 to 25 μg/mL, indicating the cell toxity could be neglected under such concentration range.

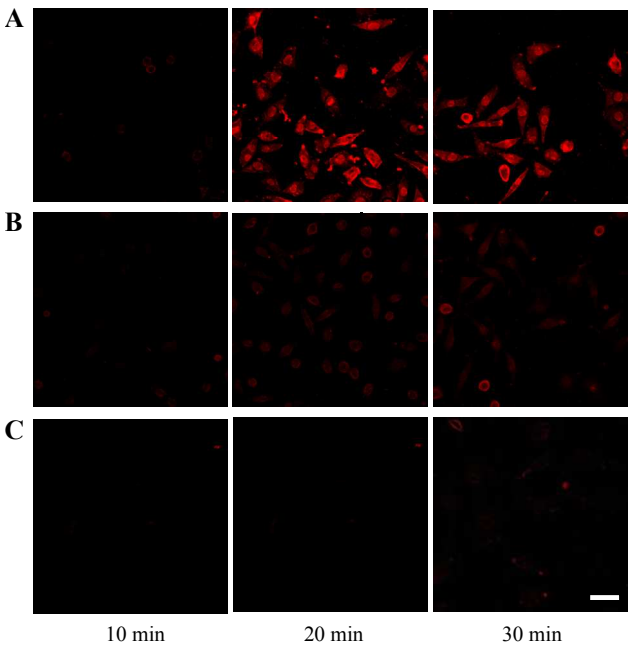

Figure 5. Time-course imaging of the cell internalization of different nanomicelles in liver cancer HepG2 cells. (A) QDs/MB nanomicelles, (B) QDs nanomicelles and (C) MB nanomicelles. Cells were incubated with the nanomicelles at 37 °C and imaged at different time intervals. (Excitation, 488 nm; Emission 660 nm long-pass filter). Bar: 10 μm.

The QDs/MB nanomicelles were further used for small animals NIR imaging. Fluorescence imaging of the mice was performed after subcutaneous injections of different nanomicelles, as the same dose QDs nanomicelles and MB nanomicelles for comparison. The nude mice were excited with 488 nm laser and the emitted fluorescence was collected in the NIR region (680−800 nm). As illustrated in Figure 6A, three different nanomicelles were carefully dipped on the buttock of the nude mice at different positions. In the present study, comparison with that of QDs and MB nanomicelles, QDs/MB nanomicelles showed the strongest brightness in the NIR region, due to high efficient FRET. A relative weak fluorescent signal could be observed for QDs nanomicelles, but no obvious fluorescence signal can be detected for MB nanomicelles. The average fluorescence intensity of different nanomicelles were further quantitative analysis. It found that QDs/MB nanomicelles was 2.43−fold higher than that of MB nanomicelles for imaging nude mice (Supporting Information). Meanwhile, it was obvious that the background fluorescence of the mice has been greatly minimized with recording in the NIR region. Therefore, our results indicated that the QDs/MB nanomicelles with a large Stokes shift demonstrated unique advantages over the MB nanomicelles in terms of increasing the contrast between the target signal and background fluorescence, which is very promising for small animals imaging.

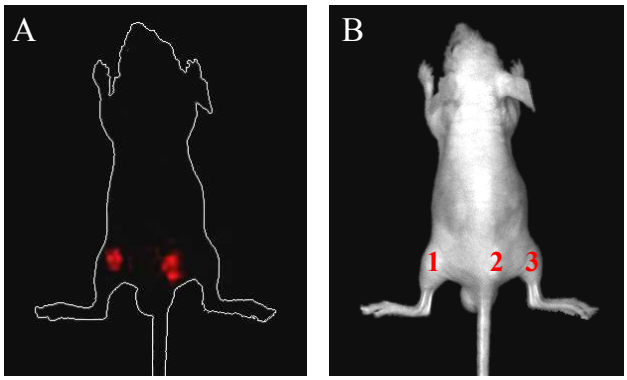

Figure 5. In vivo imaging of nude mice after subcutaneous injections with different nanomicelles. QDs nanomicelles, QDs/ MB nanomicelles, and MB nanomicelles were dipped on the buttock of the nude mice at position of 1, 2, and 3, respectively. (A) Excited at 488 nm and recorded in the NIR region (680−800 nm). (B) Bright field imaging.

In summary, by doping the QDs/MB FRET pair into the positively nanomicelles through surfactant CTAB-assistant, evaporation induced microemulsion approach, a large Stokes shifting NIR fluorescent nanoprobe was fabricated. High efficient FRET between QDs and MB rendered these nanomicelles with an enhanced fluorescence intensity, and photobleaching resistance. Meanwhile, their Stokes shift was extended to 202 nm. The nanomicelles can be rapidly internalized by cell and exhibited strong signal to background ratio in the cell and in vivo imaging. Therefore, the FRET nanomicelles could be potentially employed as an ideal fluorescence contrast agents for NIR in vivo imaging.

Acknowledgments

The authors gratefully acknowledge the financial support of the National Natural Science Foundation of China (21190040, 21322509, and 21205033), National Basic Research Program (2011CB911002), Key Technologies Research and Development Program of China (2011AA02a114).

Notes and references

[†]State Key Laboratory of Chemo/Biosensing and Chemometrics, College of Biology, College of Chemistry and Chemical Engineering, Key Laboratory for Bio-Nanotechnology and Molecular Engineering of Hunan Province, Hunan University, Changsha 410082, China.

[‡]L. Li and J.B. Liu contributed equally to this work.

[*]E-mail: kmwang@hnu.edu.cn; xiaoxiaohe@hnu.edu.cn.

References

1 H. S. Choi, S. L. Gibbs, J. H. Lee, S. H. Kim, Y. Ashitate, F. Liu, H. Hyun, G. Park, Y. Xie, S. Bae, M. Henary and J. V. Frangioni, *Nat Biotech*, 2013, **31**, 148.

2 S. H. Kim, J. H. Lee, H. Hyun, Y. Ashitate, G. Park, K. Robichaud, E. Lunsford, S. J. Lee, G. Khang and H. S. Choi, *Sci. Rep.*, 2013, **3**, 1198.

3 M.-Y. Wu, K. Li, C.-Y. Li, J.-T. Hou and X.-Q. Yu, *Chem. Commun.*, 2014, **50**, 183.

4 G. S. Filonov, K. D. Piatkevich, L.-M. Ting, J. Zhang, K. Kim and V. V. Verkhusha, *Nat Biotech*, 2011, **29**, 757.

5 H. Hyun, M. H. Park, E. A. Owens, H. Wada, M. Henary, H. J. M. Handgraaf, A. L. Vahrmeijer, J. V. Frangioni and H. S. Choi, *Nat. Med.*, 2015, **21**, 192.

6 C. Zhao, X. Li and F. Wang, *Chem. Asian J.*, 2014, **9**, 1777.

7 P. Greenspan and S. D. Fowler, *J. Lipid Res.*, 1985, **26**, 781.

8 H. S. Muddana, T. T. Morgan, J. H. Adair and P. J. Butler, *Nano Lett.*, 2009, **9**, 1559.

9 R. D. Moriarty, A. Martin, K. Adamson, E. O'Reilly, P. Mollard, R. J. Forster and T. E. Keyes, *J Microsc*, 2014, **253**, 204.

10 X. He, X. Wu, K. Wang, B. Shi and L. Hai, *Biomaterials*, 2009, **30**, 5601.

11 X. Peng, F. Song, E. Lu, Y. Wang, W. Zhou, J. Fan and Y. Gao, *J. Am. Chem. Soc.*, 2005, **127**, 4170.

12 J. Massin, W. Dayoub, J.-C. Mulatier, C. Aronica, Y. Bretonnière and C. Andraud, *Chem. Mater.*, 2011, **23**, 862.

13 X. He, K. Wang and Z. Cheng, *Wires. Nanomed. Nanobi.*, 2010, **2**, 349.

14 X. Du and Z. Y. Wang, *Chem. Commun.*, 2011, **47**, 4276.

15 X. Zhang, J. Yu, Y. Rong, F. Ye, D. T. Chiu and K. Uvdal, *Chem. Sci.*, 2013, **4**, 2143.

16 X. He, Y. Wang, K. Wang, M. Chen and S. Chen, *Anal. Chem.*, 2012, **84**, 9056.

17 J. Geng, Z. Zhu, W. Qin, L. Ma, Y. Hu, G. G. Gurzadyan, B. Z. Tang and B. Liu, *Nanoscale*, 2014, **6**, 939.

18 J. Gravier, L. Sancey, S. Hirsjärvi, E. Rustique, C. Passirani, J.-P. Benoît, J.-L. Coll and I. Texier, *Mol Pharm*, 2014, **11**, 3133.

19 Y. Jin, F. Ye, M. Zeigler, C. Wu and D. T. Chiu, *ACS Nano*, 2011, **5**, 1468.

20 L. Wang and W. Tan, *Nano Lett.*, 2006, **6**, 84.

21 X. Chen, M. C. Estévez, Z. Zhu, Y.-F. Huang, Y. Chen, L. Wang and W. Tan, *Anal. Chem.*, 2009, **81**, 7009.

22 A. Wagh, S. Y. Qian and B. Law, *Bioconjugate Chem*, 2012, **23**, 981.

23 H. Zhang and D. Zhou, *Chem. Commun.*, 2012, **48**, 5097.

24 M. Hasegawa, Y. Tsukasaki, T. Ohyanagi and T. Jin, *Chem. Commun.*, 2013, **49**, 228.

25 Y. Wang, D. Gao, P. Zhang, P. Gong, C. Chen, G. Gao and L. Cai, *Chem. Commun.*, 2014, **50**, 811.

26 Q. Ma and X. Su. *Analyst*, 2010, **135**, 1867.

27 We. Liu, H. Choi, J. P. Zimmer, E. Tanaka, J. V. Frangioni, and M. Bawendi. *J. Am. Chem. Soc.*, 2007, **129**, 14530.

28 S. Mishra, P. Kumar. J. *Adv. Eng. Res.* 2014, **1**, 36